Materials Science & Engineering C 109 (2020) 110570

Contents lists available at ScienceDirect

Materials Science & Engineering C

journal homepage: www.elsevier.com/locate/msec

Microporous carbon fibers as electroconductive immobilization matrixes: Effect of their structure on operational parameters of laccase-based amperometric biosensor

Taras Kavetskyy[a,b,*], Oleh Smutok[a,c], Olha Demkiv[a,c], Igor Maťko[d], Helena Švajdlenková[e], Ondrej Šauša[d], Ivan Novák[e], Dušan Berek[e], Katarína Čechová[d], Michal Pecz[f], Oksana Nykolaishyn-Dytso[a], Renata Wojnarowska-Nowak[g], Daniel Broda[h], Mykhailo Gonchar[a,c], Bożena Zgardzińska[i]

[a] Drohobych Ivan Franko State Pedagogical University, 82100 Drohobych, Ukraine
[b] The John Paul II Catholic University of Lublin, 20-950 Lublin, Poland
[c] Institute of Cell Biology, National Academy of Sciences of Ukraine, 79005 Lviv, Ukraine
[d] Institute of Physics, Slovak Academy of Sciences, 845 11 Bratislava, Slovakia
[e] Polymer Institute, Slovak Academy of Sciences, 845 41 Bratislava, Slovakia
[f] Faculty of Mathematics, Physics and Informatics, Comenius University in Bratislava, 842 48 Bratislava, Slovakia
[g] Center for Microelectronics and Nanotechnology, University of Rzeszow, 35-959 Rzeszow, Poland
[h] Faculty of Biotechnology, University of Rzeszow, 35-959 Rzeszow, Poland
[i] Institute of Physics, Maria Curie-Skłodowska University, 20-031 Lublin, Poland

ARTICLE INFO

Keywords:
Microporous carbon fibers
Positron annihilation
Amperometric biosensor
Laccase
Catechol
Wastewater analysis

ABSTRACT

In this study, we describe the fabrication of sensitive biosensor for the detection of phenolic substrates using laccase immobilized onto two types of microporous carbon fibers (CFs). The main characteristics of microporous CFs used for preparation of biosensors are given. Two CFs were characterized by different specific surface area, CFA (< 1 $m^2 \cdot g^{-1}$) and CFB (1448 $m^2 \cdot g^{-1}$), but with comparable size of the micropores estimated by positron annihilation lifetime spectroscopy. The structural analysis was shown that CFA is formed by thin interwoven fibers forming a highly porous structure, as well as CFB – by granular formations with uneven edges that shape a cellulose membrane of lower porosity. The results of amperometric analysis revealed that the laccase-bound CFs possesses better electrochemical behavior for laccase than non-modified rod carbon electrodes (control). Using chronoamperometric analysis, the operational parameters of the CFs-modified bioelectrodes were compared to control bioelectrodes. The bioelectrodes based on CFs have demonstrated 2.4–2.7 folds enhanced maximal current at substrate saturation (I_{max}) values, 1.2–1.4 folds increased sensitivity and twice wide linearity compared with control bioelectrodes. The sensitivity of the developed CFs-based bioelectrodes was improved compared with the laccase-bound electrodes, described in literature. The developed biosensor was tested for catechol analysis in the real communal wastewater sample.

1. Introduction

Technogenic pressure on the environment has significantly affected human health due to the pollution of water resources. Among the most dangerous pollutants of wastewater are phenolic derivates. They are classified as very toxic compounds with a high mutagenic effect for animals, as well as human. Nowadays there are stringent International standards for amount of phenol derivatives in wastewater and drinking water due to its high toxicity. The high pollution level of the natural groundwater sources is conditioned mainly by poorly treated effluents of chemical, wood and coal manufacturing, including the production of phenols, paints, resins, glues, textiles, pulp, petrochemicals, etc. [1].

The development of new methods for monitoring dangerous phenolic substances coming from the wastewater is a topical problem to improve human life first of all. The most promising analytical approach seems to be amperometric biosensors – bioanalytical devices that combine high specificity, sensitivity, reliability, portability, and simplicity in operation. Laccase is suggested to be used in biosensors to

* Corresponding author at: Drohobych Ivan Franko State Pedagogical University, 82100 Drohobych, Ukraine.
E-mail address: kavetskyy@yahoo.com (T. Kavetskyy).

https://doi.org/10.1016/j.msec.2019.110570
Received 19 September 2019; Received in revised form 22 November 2019; Accepted 17 December 2019
Available online 19 December 2019
0928-4931/

detect the wide variety of phenolic compounds, including monophenols, di-phenols, and polyphenols, as well aromatic amines. Because this enzyme does not require any exogenous cofactor in electron transfer reactions, it is a promising tool in Biosensorics. Laccase-based biosensors are very perspective in quantifying phenolic compounds with a good precision and accuracy [1–5].

The nowadays nanotechnologies open the possibility of creating bioselective elements based on nanoparticles which have unique properties not inherent to macroparticles. Nanosized materials have a high sorption capacity, ability of self-assembly and, in some cases, unique catalytic properties. Carbon materials have a very wide range of use. On the one hand, the carbon materials with a precisely defined structure, obtained by sophisticated technologies, are a hot topic for both science and industry [6]. Moreover, carbon materials derived from a very simple manufacturing process are also available and useful in many areas, for example, as a sorbents or carriers of active substances [7]. Different raw precursors for the production of such materials are often waste materials of organic origin. Among such materials there are microporous carbon fibers (CFs) prepared by carbonization of cellulose [8]. The CF prepared with a high specific surface area and particle shape enable to be a suitable carrier of the active substances on their surface. They are used, for example, as efficient sorbents for removal of chlorinated phenols [6], for decontamination of endocrine disruptors Bisphenol-A, for arsenic removal [8], etc.

In the last decade, for the development of biosensors, there are widely used a lot of carbon materials. The most popular seems to be graphene – 2D carbon nanomaterial, which has unique properties, compared with the other carbon modifications like fullerenes and carbon nanotubes [9–13]. On the other hand, direct enzyme immobilization on the surface of graphene is complicated due to its strong hydrophobicity [14]. Recently, for sensitive determination of phenolic compounds (catechol) Palanisamy et al. [15] reported the fabrication of a novel laccase-based biosensor using graphene-cellulose microfiber composite and carbon electrode. The constructed biosensor had a satisfactory selectivity showed good practicality toward catechol and phenolic compounds in different water samples. Indeed, carbon materials are of great interest to be used in bionanotechnology.

This study is focused on construction and characterization of a new mediator-less biosensor for analysis of phenolic compounds in the wastewater using laccase immobilized in the two types of microporous carbon fibers as matrixes. It was tested the relation between their structure and operational parameters of the developed biosensor.

2. Experimental

2.1. Materials (preparation)

Delignified cellulose GREENCEL purchased from Bukoza, Hencovce, Slovakia was employed without additional treatment. The oven was from Elektro, Bad Frankenhausen, Germany. In order to reduce or increase the specific surface area of samples, different methods of preparation have been chosen.

Sample CFA: Carbon microfibres prepared from delignified cellulose by carbonization without air contact at 700 °C, were boiled for 1 h in concentrated (65%) nitric acid, washed out from acid and dried.

Sample CFB: Delignified cellulose was mixed with 10 wt% solution of an activator $ZnCl_2$, who was soaked into cellulose. The resulting blend contained about 20 wt% of $ZnCl_2$, dried at 120 °C and then carbonized without contact of air oxygen at 580 °C for 1 h. Sintered coke was pulverized, washed out from $ZnCl_2$ by water and dried.

Laccase from *Trametes versicolor* with activity of ≥10 U·mg^{-1}, 2,2′-Azino-bis(3-ethylbenzthiazoline-6-sulfonic acid) (ABTS) and 99% catechol were purchased from Sigma-Aldrich (Darmstadt, Germany). The cathodic paint “GY 83-0270 0005” was from BASF Farben und Lacke (Munster, Germany).

All chemicals and reagents were prepared using triple distilled water.

2.2. Characterization of CF matrixes

2.2.1. Scanning electron microscopy (SEM)

The structure of pristine carbon fibers was investigated using high resolution JEOL JSM 6610 microscope (Tokyo, Japan). Both samples were prepared by deposition of the samples on the carbon film as a support.

2.2.2. The atomic force microscopy (AFM) and optical microscopy

AFM and optical microscopy were used for the samples size and structure characterization. The Innova AFM microscope (Bruker Corporation, Germany) was exploited. An aliquot of the tested sample was spread on the surface of freshly-cleaved mica, dried and analyzed in air using the tapping mode and super sharp TESP-SS cantilevers (Bruker). The measurements were performed with a resonance frequency of 280 kHz, scan rate of 0.2 Hz and resolution of 512 × 512 pixels.

The Leica DM 2500 M microscope (Leica Microsystems, Wetzlar, Germany) was used for obtaining optical microscopy images. The different lenses wit magnification from 5× to 100× were served for recording images.

2.2.3. Raman spectroscopy

The CFs samples were measured using inVia Micro Raman spectrometer (Renishaw, Wotton-under-Edge, UK). A series of measurements were made using different excitation wavelengths (488 nm, 633 nm, 785 nm), of which the most useful seems to be 633 nm. The laser power was set as 1.5 mW, exposure time as 10 s and 10 scans accumulations. The data were collected in the spectral range of 800–2000 cm^{-1}, with 2 cm^{-1} of spectral resolution. The samples were placed on a microscope stage (Leica DM 2500 M microscope), and a 20× lens magnification was used. The spectra were processed in the form of smoothing, baseline correction and normalization.

2.2.4. Brunauer-Emmett-Teller (BET)

A specific surface area measurement was performed on homemade glass apparatus according to Brunauer, Emmett and Teller [16]. Surface calculated from Ar adsorption at 77 K according to BET equation.

2.2.5. Positron annihilation lifetime spectroscopy (PALS)

This method was used for the estimation of pore sizes of investigated materials. Lifetime spectra were measured in air and vacuum (10^{-6} mbar) at room temperature (297 K) by the fast-fast coincidence spectrometer. The resolutions of spectrometer as well as the correction to annihilation in source of positrons were determined by aluminum defect-free sample. The LT9 program was used for the analysis of spectra [17].

Lifetimes of positron or positronium (Ps) (bonded state of electron and positron) probes, implanted to the material, depend on the density of electrons in annihilation sites and allow to estimate the hole size using an appropriate model. Very common and simple approach is the semiempirical quantum mechanical model for pick-off annihilation of *ortho*-positronium (triplet state of Ps) probe in the spherical holes [18,19]. In this case, the positron from *o*-Ps annihilate with surface electron from spherical wall with shortened lifetime of several ns compared with 142 ns lifetime of *o*-Ps in vacuum. But in some class of materials the Ps is not created or the creation is suppressed and dominant mode of annihilation is direct annihilation with lifetimes in the range of hundreds of ps. The Ps annihilation in the carbon is not observed commonly [20–23] and the pore size in the pores of such material can be estimated from second component of lifetime spectra by approach of Liao et al. [24]:

$$\tau_2 = 0.260 \times [1 - R/(R + 3.823) + (1/2\pi) \times \sin(2R/(R + 3.823))]^{-1} \quad (1)$$

where τ_2 is positron lifetime in nanoseconds and R is free-volume radius in nm. We note that the Eq. (1) is valid up to about 1 nm effective pore diameter.

2.3. Biosensors construction and characterization

2.3.1. Preparation of CFs for biosensor construction

1 mL of acetone was added to 14 mg of solid CFs and ultrasonicated for 1 min. The prepared suspensions of CFs were used for modification of 3.05 mm graphite-rod electrodes.

2.3.2. Construction of amperometric biosensor

For construction of the laccase-based amperometric biosensors, graphite electrodes were previously modified by dropping 5 μL CFs suspensions. After formation of CFs films, 5 μL aliquot of a prepared enzyme solution (laccase from *Trametes versicolor*; 50 mM acetate buffer, pH 4.5 with activity 50 U·mL^{-1}) was dropped on the working electrode surface and the formed layer of CFs-enzyme was covered with cathodic paint "GY 83-0270 0005" [25].

The enzyme-modified graphite electrodes without CFs-modification were used as a control.

The prepared bio-functionalized electrodes were rinsed with 50 mM acetate buffer, pH 4.5 and kept at 4 °C till usage.

2.3.3. Amperometric measurements

The amperometric biosensors were constructed in a three-electrode configuration using constant-potential amperometry. The biosensor configuration included a Pt counter electrode, Ag/AgCl/KCl reference electrode, and a graphite-rod working electrode. The graphite rods (type RW001, 3.05 mm) from Ringsdorff Werke (Bonn, Germany) were used as working electrodes. Before usage, the electrodes were polished with emery paper. The amperometric analysis was carried out using a potentiostat CHI 1200A (IJ Cambria Scientific, Burry Port, UK) in an electrochemical cell at 25 °C under continuous stirring.

Cyclic voltamperometric analysis of control (non-modified) and modified with CFs graphite-rod electrodes was performed with scan rate 50 mV·s^{-1} vs Ag/AgCl (reference electrode) in electrolyte solution consisting of 10 mM $K_4Fe(CN)_6$ and 100 mM KCl. Cyclic voltamperometric analysis of control and CFs-modified laccase based bioelectrodes was done with scan rate 10 mV·s^{-1} vs Ag/AgCl in 50 mM acetate buffer, pH 4.5 at 23 °C.

Chronoamperometric analysis of control and CFs-modified laccase-based bioelectrodes was performed with working potential 0.0 mV vs Ag/AgCl in 50 mM acetate buffer, pH 4.5 at 23 °C and constant stirring using a magnetic mixer.

2.4. Real samples analysis

2.4.1. HPLC-DAD analysis

The raw communal wastewater, as well as spiked samples, were analyzed using high-performance liquid chromatography (HPLC) Dionex system equipped (Sunnyvale, USA) with a pump with degasser (UltiMate 3000 Pump), an auto sampler (UltiMate 3000 Autosampler), a column oven (UltiMate 3000 Column Compartment), and multi-wavelength detector (UltiMate 3000 RS Diode Array Detector). The assay was performed using column NovaPak® C18, 4 μm 3.9 × 150 mm, under the next conditions: eluent A – acetonitrile; eluent B – water; the mobile phase was acetonitrile-water (40:60, v/v) under isocratic conditions; flow rate 1.0 mL·min^{-1}; temperature 40 °C; injection volume 20 μL; detection at λ_1 = 228 nm. As a stock solution was used 25 mM catechol in methanol (9:1 v/v), as a working solution – 0.25 mM catechol in methanol. Prior analysis, the raw wastewater sample was filtered through millipore 0.45 μm filter.

2.4.2. Biosensor analysis

Analysis of the real wastewater samples by CFA-modified bioelectrode was performed using "*standard addition mode*", a proven measurement method in a complex sample matrix [26].

3. Results and discussion

3.1. Preparation and characterization of carbon fibers

Two different types of carbon fibers (CFs) prepared by carbonization of cellulose were selected for the test of their properties in untreated condition as well as a biosensor composite. The differences between them were mainly in the specific surface area and in their preparation process. To estimate the structure and size of the particles of CFA and CFB samples, AFM analysis was performed. For this, the CFs samples were suspended and disintegrated in acetone before fixation on the mica surface, in the same way as for the preparation of CFs suspension for biosensor construction (0.1 mL acetone was added to 1.4 mg solid CFs and ultrasonicated for 1 min). Unfortunately, the particles of the treated CFs were too large with a high roughness to be well scanned by AFM. Because of the large size of the studied CFA and CFB structural particles, we have analyzed them by means of ultramicrophotography using Leica DM 2500 M optical microscope (see supplementary material Fig. S1).

The detail structural characterization of the CFA and CFB samples was performed using SEM analysis (Fig. 1). The SEM analysis has confirmed previous ultramicrophotography results: CFA is formed by thin interwoven fibers (with the width about 10–15 μm and lengths from several dozen to several hundred microns) forming a highly

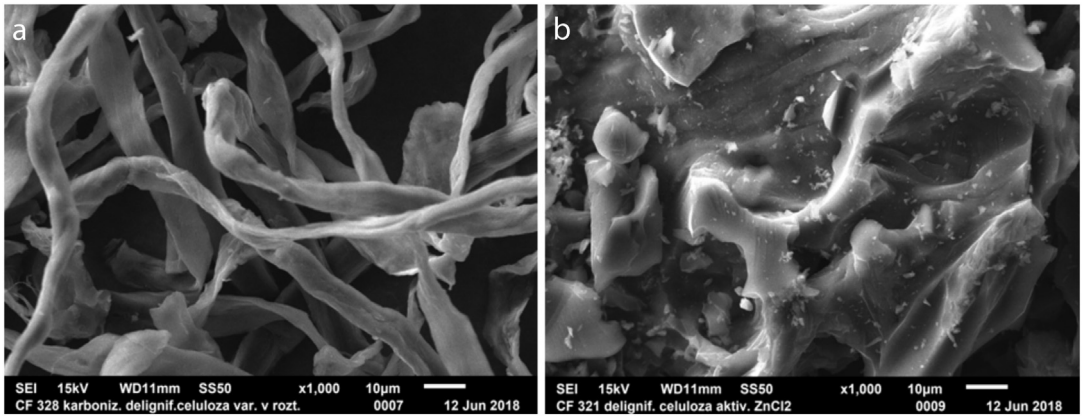

Fig. 1. Scanning electron microscopy of the CFA (left) and CFB (right). *Note:* kV – accelerating voltage; WD – distance from the last lens of microscope to the samples (mm); SS – spot size (probe current); x – fold magnification; μm – scale unit.

Table 1
The quantities specific surface area SSA, second lifetime component τ_2, calculated free-volume hole radius R_h as well as consistency and precursors used for the investigated pristine CF samples.

Sample	SSA (BET), $m^2 \cdot g^{-1}$	τ_2, ns	R_h, nm	I_2, %	Consistency	Precursors
CFA	< 1	0.452 (0.004)	0.33 (0.01)	89.2 (0.6)	Microfibres	Delignified cellulose
CFB	1448	0.395 (0.002)	0.28 (0.01)	89.3 (0.6)	Microfibres in flat scales	Delignified cellulose, $ZnCl_2$ activator

porous structure, as well CFB – by granular formations with uneven edges (the size from 90 μm × 60 μm up to 230 μm × 160 μm) forming a cellulose membrane of lower porosity. Obtained results are consistent with the results of SSA (BET) analysis represented in Table 1.

Despite the large difference in the specific surface area, the difference in the size of the micropores estimated by PALS is not large. CFB sample has smaller micropores in comparison with CFA. This statement is based on the following facts. Time spectra were described by two lifetime components in region of hundreds of ps, at room temperature (298 K) and vacuum (10^{-5} mbar). The long time component in the ns region was not observed to indicate positronium formation. The 2-component decomposition of the positron lifetime spectra into discrete components using the LT program gave approximately the same short component for both materials with the value (188 ± 4 ps) and the very intense second component, which is in Table 1. We assume that the first component comes from the skeleton of fibers, and is in good agreement with the values of bulk component reported in the literature for various carbon materials in the 170–202 ps range [21]. The defective structure is generally manifested by prolonging the lifetime, since there is a reduced electron density. Therefore, we assume that the second component of the time spectra originates from the micropore structure and the fiber surface. Its value varies depending on the average free-spaces. We do not assume that it is a regular structure that could have a similar lifetime as C_{60} (356–359 ps [21,22]) and is attributed to electron annihilation near the octahedral sites of fcc lattices. In our case, amorphous structures were confirmed by XRD measurements. Carbon fibers produced from polyacrylonitrile precursor exhibited lifetimes of a similar range of 373–441 ps [27].

The mean pore size was determined from the measured lifetimes of positrons in such a micropore structure (τ_2, Table 1). Their size was estimated using Eq. (1).

If we suppose that number of micropores is proportional to the relative intensity of second lifetime component, we can conclude that in this case the concentration of micropores is similar in both samples. The intensity I_2 is very high and since the third component has not been found in the lifetime spectra of both types of CF, this indicates trapping of positrons practically in one type of defects or open spaces.

The sorption ability of CFA and CFB samples for the water is 12.5% and 60.0%, respectively.

The CFA and CFB samples were additionally characterized using Raman spectroscopy (Fig. 2).

Both of CFs have demonstrated two intensive peaks characteristic for carbon structures. D-band corresponds to the defect-induced mode and G-band is associated with the vibration of sp^2-bonded carbon atoms in a 2D hexagonal lattice [28]. The D-band occurs at 1339 cm^{-1} and 1354 cm^{-1} for CFA and CFB sample, respectively. The position of G-band is similar in both samples (1595 cm^{-1}, 1593 cm^{-1}) (Fig. 2). The presence of the bands reveals the occurrence of C sp^2 atoms in benzene or condensed benzene rings of amorphous (partially hydrogenated) carbon [28]. The noticeable shift of D-band occurs due to the different formation of carbon materials, including the change in the mechanical constant of the C—C bond [29]. The intensity ratio of the D-band to G-band in the investigated sample is slightly different. The I_D/I_G ratio of the CFB sample was 0.75, and it is lower than that of CFA (I_D/I_G = 0.82), indicating the reduced disorder degree of the materials. The crystalline structure could provide an orderly charge transfer path,

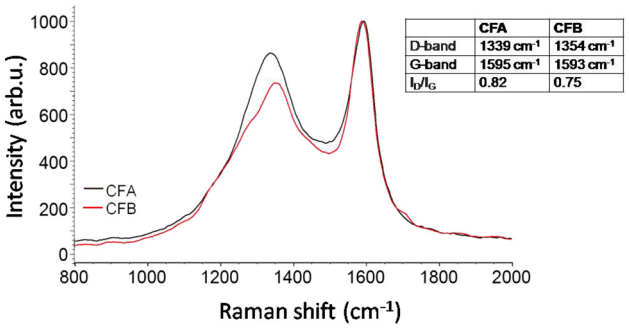

Fig. 2. Raman spectra of CFA (black line) and CFB (red line) samples, λ = 633 nm. (For interpretation of the references to colour in this figure legend, the reader is referred to the web version of this article.)

resulting in a good electrical conductivity, with a faster response time [30].

3.2. Construction and characterization of CFs-based laccase biosensors

The enzyme laccase (polyphenol oxidase from *Trametes versicolor*; EC 1.10.3.2) is a member of the blue multi-copper-oxidase family. The enzyme has been studied for a long time, due to its ability to oxidize a number of organic substrates and to reduce molecular oxygen to water [31]. Laccase is made up of a cluster of four copper atoms (type I copper; type II copper and two type III copper atoms) that form the active site of the enzyme [32]. The copper consisting cluster provides the ability of laccase to direct electron transfer from reduced enzyme to a surface of carbon electrodes [33]. This ability of some enzymes to direct electron transfer is widely used in construction of the novel biosensors and biofuel cells [34,35].

We have used laccase, coupled with CFs-modified graphite-rod electrodes, for construction of a new mediator-less biosensor for analysis of phenolic compounds. To estimate the impact of two types of CFs (marked as CFA and CFB) on the efficiency of electron transfer through graphite-rod electrode, the cyclic voltamperometry analysis was performed (Fig. 3).

The cyclic voltamperometry analysis using ferri/ferrocyanide redox couple revealed that the modification of the graphite-rod electrode with CFs greatly enhanced the efficiency of electron transfer due to an increase of electrochemically accessible electrode surface area (Fig. 3).

To determine an optimal working potential for the laccase-based biosensors, the cyclic voltamperometric analysis was performed using ABTS (see supplementary material Fig. S2), as well as catechol (Fig. S3) as typical laccase substrates in acetate buffer, pH 4.5 which is optimal for laccase from *Trametes versicolor* [36]. The amperometric detection is based on a reduction of oxidized electroactive products (probably, for ABTS – cation-radicals $ABTS^{+\cdot}$ and $ABTS^{2(+\cdot)}$; for catechol – semi-quinone intermediate) formed in laccase enzymatic reaction (see supplementary material Fig. S4). Fig. S2 shows a cyclic voltamperometric response of the different types of laccase-based bioelectrodes constructed using CFA- and CFB-modified graphite-rod electrodes without and in presence of ABTS. As shown, there is a well resolved redox peak at the addition of ABTS. An increasing the reduction peak testifies brightly the high efficiency of the electron transfer between

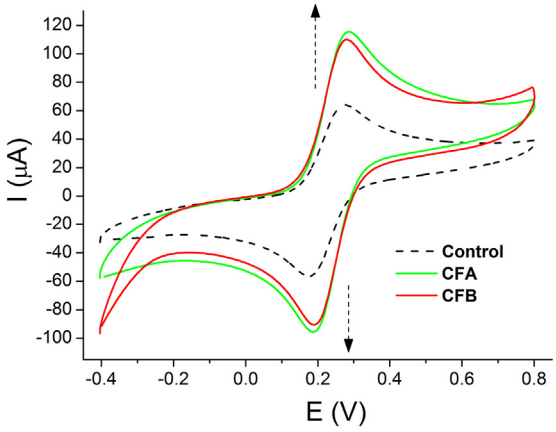

Fig. 3. Cyclic voltamperograms of control (non-modified) and modified with CFs graphite-rod electrodes: dash line – control; green solid line – CFA-modified; red solid line – CFB-modified. (For interpretation of the references to colour in this figure legend, the reader is referred to the web version of this article.)

electroactive product of laccase reaction and the CFs-modified surface of the transducer. Moreover, it allows estimating an optimal working potential for the biosensors, which corresponds to 0.0 mV versus Ag/AgCl. The working potential close to 0.0 mV vs Ag/AgCl makes the biosensor more selective, due to avoiding interference reactions of electroactive chemicals presented in the real samples which can run at extreme values of the working potential.

The mentioned above potential was selected for further work on the study of characteristics of the constructed bioelectrodes. On the other hand, cyclic voltamperometric analysis gives us the preliminary information about efficiency of electron transfer through the transducer and enzymatically oxidized product to laccase immobilized onto non-modified and CFA- and CFB-modified bioelectrodes.

The Figs. S2 and S3 of supplementary material demonstrate significantly difference in amperometric outputs for different bioelectrodes at the same ABTS or catechol concentration which tightly depend on the efficiency of electron transfer. The non-modified bioelectrode (control) has shown 1.0 μA output on 0.5 mM ABTS. The CFs-modified bioelectrodes have demonstrated up to 1.85-fold (1.85 μA, CFA) and 2.3-fold (2.3 μA, CFB) higher output compared with the control bioelectrode (Fig. S2). The increase of the cyclic voltamperometric response for CFs-modified bioelectrodes in the presence of catechol was also observed (Fig. S3). The control bioelectrode has shown 1.1 μA output on 0.5 mM catechol. The CFs-modified bioelectrodes at the potential 0.0 mV have demonstrated a higher output up to 1.45-fold (1.6 μA, CFA) and 2-fold (2.2 μA, CFB) compared with the control bioelectrode, respectively.

For more detailed characterization of the biosensors, chronoamperometric analysis was performed using ABTS, as well catechol (Fig. 4 and Figs. S5, S6) as substrates.

Fig. S5 shows chronoamperograms of the control and CFs-modified bioelectrodes. Following to the chronoamperograms of the bioelectrodes obtained, calibration curves of response on the increasing concentration of ABTS was plotted as illustrated in Fig. 4 (left). As seen from the calibration curve, the control bioelectrode response (maximal current at substrate saturation I_{max}) was estimated to be 3.15 ± 0.1 μA and the apparent Michaelis-Menten constant (K_M^{app}) to ABTS was 0.11 ± 0.01 mM. The I_{max} values are 8.5 ± 0.3 μA, and 7.5 ± 0.2 μA for CFA- and CFB-modified bioelectrodes, respectively. The value of K_M^{app} was estimated as 0.35 ± 0.03 mM and 0.2 ± 0.01 mM of ABTS (for CFA- and CFB-based bioelectrodes, respectively). The obtained 2.7-fold higher I_{max} value for CFA- and 2.4-fold for CFB-modified bioelectrode indicate a higher electroconductivity of bioselective membrane, compared with control bioelectrode. The detection limit to ABTS for the biosensors was calculated as 2 μM.

Chronoamperometric responses of control and modified by CFs laccase-based bioelectrodes toward catechol are presented in Fig. S6 and the corresponding calibration curves in Fig. 4 (right). The I_{max} value for catechol response for both types of CFs-modified bioelectrodes was estimated as 3.9 ± 0.1 μA. The control bioelectrode demonstrated 1.2-fold lower I_{max} value. Moreover, K_M^{app} for catechol for both bioelectrodes modified by CFs was quite the same (0.45 ± 0.01 and 0.49 ± 0.01 mM) and 1.2–1.3-fold decreased compared to control bioelectrode (0.6 ± 0.04 mM). The increased substrate affinity of CFs-modified bioelectrodes additionally indicates a high efficiency of electron transferring between the electroactive enzymatic products, CFs, and surface of the transducer. The detection limit to catechol for both biosensors was less 5 μM.

The linearity of calibration curves for ABTS is in the frames from 0.01 to 0.2 mM CFA- and 0.01–0.1 mM for CFB-modified bioelectrodes. The linearity for the control bioelectrode was significantly shorter – from 0.01 to 0.05 mM (Fig. 5).

The sensitivity of the bioelectrodes to different substrates was calculated from the slope of the calibration curves (*B*) considering a working area of the electrode used (7.3 mm^2). The sensitivity of the control bioelectrode for ABTS is equal to 1986 $A{\cdot}M^{-1}{\cdot}m^{-2}$. In the case of modified bioelectrodes, the sensitivity to ABTS corresponds to 2890 $A{\cdot}M^{-1}{\cdot}m^{-2}$ and 4096 $A{\cdot}M^{-1}{\cdot}m^{-2}$ for CFA- and CFB-modified electrodes, respectively (Fig. 5, left). The analysis of sensitivity of the bioelectrodes to catechol is presented in Fig. 5 (right). The control bioelectrode demonstrated a sensitivity of 685 $A{\cdot}M^{-1}{\cdot}m^{-2}$ to catechol, in contrast to 1000 $A{\cdot}M^{-1}{\cdot}m^{-2}$ for CFA- and 1137 $A{\cdot}M^{-1}{\cdot}m^{-2}$ for CFB-modified bioelectrodes. The substrate sensitivity of the developed CFs-based bioelectrodes was improved compared with the described in literature laccase-based 3.05 mm graphite-rod electrodes – 5.2 $A{\cdot}M^{-1}{\cdot}m^{-2}$ for ABTS and 3.3 $A{\cdot}M^{-1}{\cdot}m^{-2}$ for catechol [37], laccase-modified 3.0 mm glassy carbon electrodes – 358.3 $A{\cdot}M^{-1}{\cdot}m^{-2}$ for ABTS and 970.5 $A{\cdot}M^{-1}{\cdot}m^{-2}$ for catechol [38], reduced graphene oxide-glycol chitosan nanohybrid – 93 $A{\cdot}M^{-1}{\cdot}m^{-2}$ for catechol [39], and graphene-cellulose microfiber composite modified carbon screen-printed electrodes – 932 $A{\cdot}M^{-1}{\cdot}m^{-2}$ for catechol [15].

3.3. Analysis of the real wastewater samples

The developed CFA-modified bioelectrodes were used for analysis of catechol in a communal wastewater sample that has been collected at the treatment plant of Rzeszow (Poland) prior to its purification. There were tested the raw and spiked wastewater samples. The spiked samples were made by the addition of the tested analyte (catechol) in 0.25 mM concentration to the raw wastewater. The biosensor analysis was performed using "*standard addition mode*" (Fig. S7) and obtained results were compared with results of HPLC analysis (Fig. S8) of the same samples (Table 2).

HPLC analysis of the tested wastewater samples (raw and spiked) showed that a raw sample contained a number of components (Fig. S8), one of them is close to catechol (retention time is 1.34 vs 1.39 min for added catechol), with a content estimated to be 0.043 ± 0.004 mM. For sample, spiked with 0.25 mM catechol, HPLC analysis revealed practically the same value (0.2498 ± 0.001 mM). So, contaminant with retention time of 1.34 min would not be really catechol. Taking into account this conclusion, there is consequent a high coincidence of the obtained values (recovery value is close to 100%).

The biosensor analysis demonstrated the following results for catechol content in the tested samples: 0.108 ± 0.03 mM (a raw wastewater) and 0.359 ± 0.05 mM (a sample spiked with 0.25 mM catechol) (Fig. S7). This testifies a high recovery (100.3%) of catechol spiked with wastewater sample (0.108 + added 0.25 mM). The real samples analysis has shown an absence of any interfering impact of the compounds of raw wastewater on biosensor analysis. Moreover, the slope for "*standard addition mode*" calibration of raw wastewater was

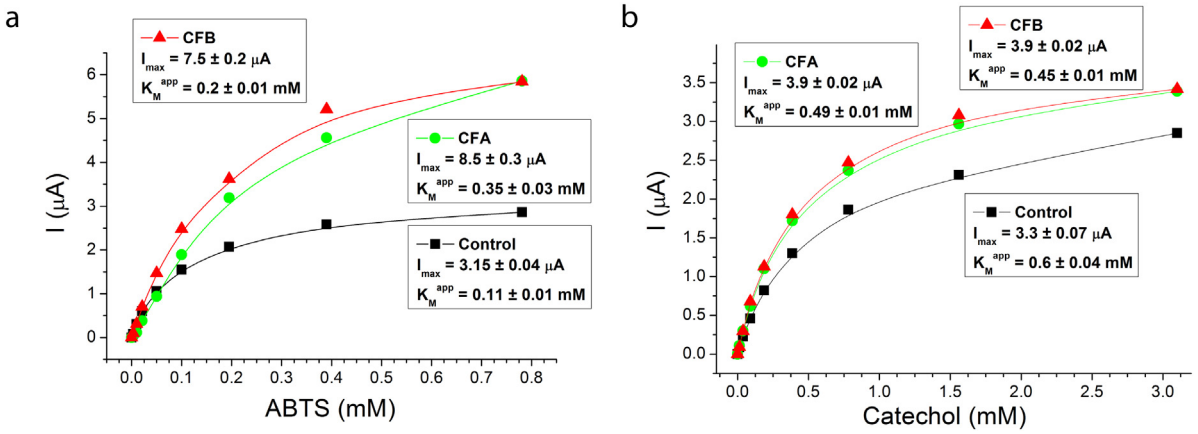

Fig. 4. Calibration curves of chronoamperometric response onto the increasing concentrations of ABTS (left) and catechol (right) for the control, and CFs-modified bioelectrodes.

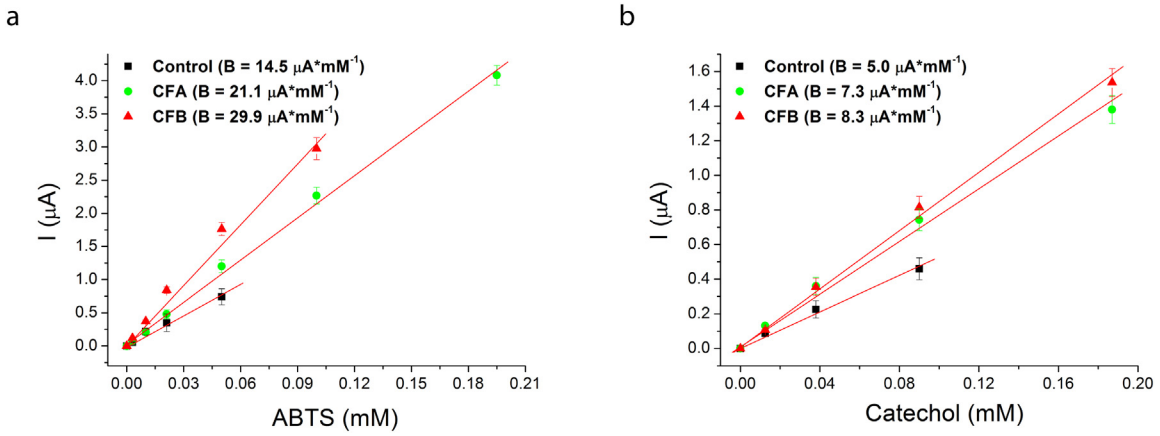

Fig. 5. Sensitivity analysis of the non-modified (control) and CFs-modified bioelectrodes for ABTS (left) and catechol (right). Abbreviations: *B* – current slope at a working electrode diameter of 3.05 mm.

Table 2
Quantitative catechol assay in wastewater samples by biosensor and HPLC methods.

Sample	Biosensor, mM	HPLC, mM
Raw wastewater	0.108 ± 0.03	0.043 ± 0.004
Spiked wastewater	0.359 ± 0.05	0.2498 ± 0.001

calculated as 5.54 ± 0.29 mA·mM^{-1} that is quite similar to a slope of calibration curve obtained for catechol standard solution (5.6 ± 0.4 mA·mM^{-1}) (Fig. S7). This demonstrates a high accuracy of biosensor analysis of real communal wastewater samples.

A significant difference between analytical results obtained by biosensor and HPLC approaches (Table 2) is hardly explainable. It seems that the real sample contains some catechol-like components which are oxidizable by a not very specific laccase. On the other hand, so broad specificity of laccase allows estimating a broader range of toxicants that is very important for fast and simple monitoring of wastewater by biosensor.

4. Conclusions

The sensitive biosensor for the detection of phenolic substrates using laccase immobilized on the two types of microporous carbon fibers (CFs) has been developed. The CFs are characterized by different specific surface area, CFA (< 1 m^2·g^{-1}) and CFB (1448 m^2·g^{-1}), but with a comparable size of the micropores estimated by positron annihilation lifetime spectroscopy. The structural analysis was shown that CFA is formed by thin interwoven fibers forming a highly porous structure, as well as CFB – by granular formations with uneven edges that shape a cellulose membrane of lower porosity. The cyclic voltammetry results revealed that the laccase immobilized on CFs is characterized by improved bioanalytical properties, compared with control (without CFs). Using chronoamperometric analysis the operational parameters of the CFs-modified bioelectrodes, compared with control bioelectrode were estimated. The bioelectrodes based on CFs have demonstrated 2.4–2.7-fold enhanced I_{max} values, 1.2–1.4-fold increased sensitivity and twice wide linearity compared with control bioelectrode.

An enhanced sensitivity and a wider linearity for both substrates (ABTS and catechol) make the developed CFs-based laccase biosensors more promising for the estimation of phenolic contaminants in samples (e.g., drinking water or groundwater) where their content is very low.

The developed biosensors were tested for catechol analysis in the real communal wastewater sample.

Authors' contributions

Dr. T. Kavetskyy conceived of the study, participated in its design, coordination and wrote the manuscript. Dr. O. Smutok and Dr. O. Demkiv performed the immobilization experiment, voltammetry and amperometric measurements and drafted the manuscript. Dr. I. Maťko, Dr. H. Švajdlenková, Dr. I. Novák, and Dr. D. Berek prepared the microporous carbon fibers used for the research, performed microscopy

experiment and drafted the manuscript. Dr. O. Šauša, K. Čechová, and M. Pecz performed the positron annihilation lifetime spectroscopy measurements and drafted the manuscript. Dr. O. Nykolaishyn-Dytso participated in the sequence alignment, experimental data treatment and drafted the manuscript. Dr. R. Wojnarowska-Nowak performed the optical microscopy and Raman spectroscopy measurements and drafted the manuscript. Dr. D. Broda performed the HPLC experiment and drafted the manuscript. Prof. M. Gonchar supervised the research and drafted the manuscript. Dr. B. Zgardzińska participated in the positron annihilation lifetime spectroscopy data treatment and real sample analysis and drafted the manuscript. All authors read and approved the final manuscript.

Declaration of competing interest

The authors declare that they have no known competing financial interests or personal relationships that could have appeared to influence the work reported in this paper.

Acknowledgements

This work was supported in part by the Ministry of Education and Science of Ukraine (projects Nos. 0118U000297 and 0119U100671), National Academy of Sciences of Ukraine in the frame of the Scientific-Technical Program “Smart sensor devices of a new generation based on modern materials and technologies” (project No. 13), and Slovak Grant Agency VEGA (projects Nos. 2/0157/17 and 2/0127/17). T.K. also acknowledges the SAIA (Slovak Academic Information Agency) for scholarship in the IPSAS within the National Scholarship Programme of the Slovak Republic.

Appendix A. Supplementary data

Supplementary data to this article can be found online at https://doi.org/10.1016/j.msec.2019.110570.

References

[1] M.M. Rodríguez-Delgado, G.S. Alemán-Nava, J.M. Rodríguez-Delgado, G. Dieck-Assad, S.O. Martínez-Chapa, D. Barceló, R. Parra, Laccase-based biosensors for detection of phenolic compounds, Trends Anal. Chem. 74 (2015) 21–45, https://doi.org/10.1016/j.trac.2015.05.008.

[2] E. Casero, M.D. Petit-Domínguez, L. Vázquez, I. Ramírez-Asperilla, A.M. Parra-Alfambra, F. Pariente, E. Lorenzo, Laccase biosensors based on different enzyme immobilization strategies for phenolic compounds determination, Talanta 115 (2013) 401–408, https://doi.org/10.1016/j.talanta.2013.05.045.

[3] P. Das, L. Barbora, M. Das, P. Goswami, Highly sensitive and stable laccase based amperometric biosensor developed on nano-composite matrix for detecting pyrocatechol in environmental samples, Sensors Actuators B Chem. 192 (2014) 737–744, https://doi.org/10.1016/j.snb.2013.11.021.

[4] X. Xu, M. Guo, P. Lu, R. Wang, Development of amperometric laccase biosensor through immobilizing enzyme incopper-containing ordered mesoporous carbon (Cu-OMC)/chitosan matrix, Mater. Sci. Eng. C 30 (2010) 722–729, https://doi.org/10.1016/j.msec.2010.03.006.

[5] M. Ardhaoui, S. Bhatt, M. Zheng, D. Dowling, C. Jolivalt, F.A. Khonsari, Biosensor based on laccase immobilized on plasma polymerizedallylamine/carbon electrode, Mater. Sci. Eng. C 33 (2013) 3197–3205, https://doi.org/10.1016/j.msec.2013.03.052.

[6] E.B. Simsek, I. Novak, O. Sausa, D. Berek, Microporous carbon fibers prepared from cellulose as efficient sorbents for removal of chlorinated phenols, Res. Chem. Intermed. 43 (2017) 503–522, https://doi.org/10.1007/s11164-016-2637-1.

[7] E.B. Simsek, D. Saloglu, N. Ozcan, I. Novak, D. Berek, Carbon fiber embedded chitosan/PVA composites for decontamination of endocrine disruptor bisphenol-A from water, J. Taiwan Inst. Chem. Eng. 70 (2017) 291–301, https://doi.org/10.1016/j.jtice.2016.11.008.

[8] E.B. Simsek, I. Novak, D. Berek, U. Beker, Novel composite sorbents based on carbon fibers decorated with ferric hydroxides – arsenic removal, Asia Pac. J. Chem. Eng. (2018) e2237, , https://doi.org/10.1002/apj.2237.

[9] Y. Shao, J. Wang, H. Wu, J. Liu, I.A. Aksay, Y. Lin, Graphene based electrochemical sensors and biosensors: a review, Electroanalysis 22 (2010) 1027–1036, https://doi.org/10.1002/elan.200900571.

[10] T. Kuila, S. Bose, A.K. Mishra, P. Khanra, N.H. Kim, J.H. Lee, Chemical functionalization of graphene and its applications, Prog. Mater. Sci. 57 (2012) 1061–1105, https://doi.org/10.1016/j.pmatsci.2012.03.002.

[11] I.V. Pavlidis, M.P. Patila, U.T. Bornscheuer, D. Gournis, H. Stamatis, Graphene-based nanobiocatalytic systems: recent advances and future prospects, Trends Biotechnol. 32 (2014) 312–320, https://doi.org/10.1016/j.tibtech.2014.04.004.

[12] R. Pang, M. Li, C. Zhang, Degradation of phenolic compounds by laccase immobilized on carbon nanomaterials: diffusional limitation investigation, Talanta 131 (2015) 38–45, https://doi.org/10.1016/j.talanta.2014.07.045.

[13] J. Barkauskas, L. Mikoliunaite, I. Paklonskaite, P. Genys, J.J. Petroniene, I. Morkvenaite-Vilkonciene, A. Ramanaviciene, U. Samukaite-Bubniene, A. Ramanavicius, Single-walled carbon nanotube based coating modified with reduced graphene oxide for the design of amperometric biosensors, Mater. Sci. Eng. C 98 (2019) 515–523, https://doi.org/10.1016/j.msec.2019.01.005.

[14] C. Karuppiah, S. Palanisamy, S.M. Chen, V. Veeramani, P.A. Periakaruppan, A novel enzymatic glucose biosensor and sensitive non-enzymatic hydrogen peroxide sensor based on graphene and cobalt oxide nanoparticles composite modified glassy carbon electrode, Sensors Actuators B Chem. 196 (2014) 450–456, https://doi.org/10.1016/j.snb.2014.02.034.

[15] S. Palanisamy, S.K. Ramaraj, S.M. Chen, T.C. Yang, P. Yi-Fan, T.W. Chen, V. Velusamy, S. Selvam, A novel laccase biosensor based on laccase immobilized graphene-cellulose microfiber composite modified screen-printed carbon electrode for sensitive determination of catechol, Sci. Rep. 7 (2017) 41214, , https://doi.org/10.1038/srep41214.

[16] S. Brunauer, P. Emmett, E. Teller, Adsorption of gases in multimolecular layer, J. Am. Chem. Soc. 60 (1938) 309–319, https://doi.org/10.1021/ja01269a023.

[17] J. Kansy, Microcomputer program for analysis of positron annihilation lifetime spectra, Nucl. Instrum. Meth. A 374 (1996) 235–244, https://doi.org/10.1016/0168-9002(96)00075-7.

[18] S.J. Tao, Positronium annihilation in molecular substances, J. Chem. Phys. 56 (1972) 5499–5510, https://doi.org/10.1063/1.1677067.

[19] M. Eldrup, D. Lightbody, J.N. Sherwood, The temperature dependence of positron lifetimes in solid pivalic acid, Chem. Phys. 63 (1981) 51–58, https://doi.org/10.1016/0301-0104(81)80307-2.

[20] T. Azuma, H. Saito, Y. Yamazaki, K. Komaki, Y. Nagashima, H. Watanabe, T. Hyodo, H. Kataura, N. Kobayashi, Positron lifetime in C_{60}/C_{70} powder, J. Phys. Soc. Jpn. 60 (1991) 2812–2814, https://doi.org/10.1143/JPSJ.60.2812.

[21] Y.C. Jean, X. Lu, Y. Lou, A. Bharathi, C.S. Sundar, Y. Lyu, P.H. Hor, C.W. Chu, Positron annihilation in C_{60}, Phys. Rev. B 45 (1992) 12126–12129, https://doi.org/10.1103/physrevb.45.12126.

[22] J. Krištiak, K. Krištiakova, O. Šauša, Phase transition in C_{60} observed by positron annihilation, Phys. Rev. B 50 (1994) 2792–2794, https://doi.org/10.1103/physrevb.50.2792.

[23] F. Becvar, I. Novotny, I. Prochazka, D. Rafaja, J. Kern, Positron lifetimes for neutron-irradiated C_{60}, Appl. Phys. A Mater. Sci. Process. 61 (1995) 335–337, https://doi.org/10.1007/BF01538200.

[24] K.-S. Liao, H. Chen, S. Awad, J.-P. Yuan, W.-S. Hung, K.-R. Lee, J.-Y. Lai, C.-C. Hu, Y.C. Jean, Determination of free-volume properties in polymers without orthopositronium components in positron annihilation lifetime spectroscopy, Macromolecules 44 (2011) 6818–6826, https://doi.org/10.1021/ma201324k.

[25] M. Karkovska, O. Smutok, N. Stasyuk, M. Gonchar, L-lactate-selective microbial sensor based on flavocytochrome b_2-enriched yeast cells using recombinant and nanotechnology approaches, Talanta 144 (2015) 1195–1200, https://doi.org/10.1016/j.talanta.2015.07.081.

[26] R.B. Graham, S.G. Paramjit, Estimates of precision in a standard addition analysis, J. Chem. Educ. 76 (1999) 805–807, https://doi.org/10.1021/ed076p805.

[27] J. Dryzek, E. Pamula, S. Blazewicz, Positron annihilation in carbon fibers, Phys. Status Solidi (a) 151 (1995) 39–46, https://doi.org/10.1002/pssa.2211510106.

[28] M. Sevilla, A.B. Fuertes, The production of carbon materials by hydrothermal carbonization of cellulose, Carbon 47 (2009) 2281–2289, https://doi.org/10.1016/j.carbon.2009.04.026.

[29] X. Ma, C. Yuan, X. Liu, Mechanical, microstructure and surface characterizations of carbon fibers prepared from cellulose after liquefying and curing, Materials 7 (2014) 75–84, https://doi.org/10.3390/ma7010075.

[30] B. Nasri-Nasrabadi, A. Kaynak, Z. Komeily-Nia, S.D. Adams, J. Li, A.Z. Kouzani, Surface nanogrooving of carbon microtubes, Sci. Rep. 8 (2018) 9924, https://doi.org/10.1038/s41598-018-28313-0.

[31] E.I. Solomon, U.M. Sundaram, T.E. Machonkin, Multicopper oxidases and oxygenases, Chem. Rev. 96 (1996) 2563–2605, https://doi.org/10.1021/cr950046o.

[32] T. Piontek, K. Antorini, M. Choinowski, Crystal structure of a laccase from the fungus *Trametes versicolor* at 1.90-a resolution containing a full complement of coppers, J. Biol. Chem. 227 (2002) 37663–37669, https://doi.org/10.1074/jbc.M204571200.

[33] S. Shleev, A. Jarosz-Wilkolazka, A. Khalunina, O. Morozova, A. Yaropolov, T. Ruzgas, L. Gorton, Direct electron transfer reactions of laccases from different origins on carbon electrodes, Bioelectrochemistry 67 (2005) 115–124, https://doi.org/10.1016/j.bioelechem.2005.02.004.

[34] G. Bagdžiūnas, A. Ramanavičius, Towards direct enzyme wiring: a theoretical investigation of charge carrier transfer mechanisms between glucose oxidase and organic semiconductors, Phys. Chem. Chem. Phys. 21 (2019) 2968–2976, https://doi.org/10.1039/c8cp07233g.

[35] A. Ramanavicius, A. Kausaite, A. Ramanaviciene, Enzymatic biofuel cell based on anode and cathode powered by ethanol, Biosens. Bioelectron. 24 (2008) 761–766, https://doi.org/10.1016/j.bios.2008.06.048.

[36] I. Stoilova, A. Krastanov, V. Stanchev, Properties of crude laccase from *Trametes versicolor* produced by solid-substrate fermentation, Adv. Biosci. Biotechnol. 1 (2010) 208–215, https://doi.org/10.4236/abb.2010.13029.

[37] A. Jarosz-Wilkołazka, T. Ruzgas, L. Gorton, Amperometric detection of mono- and diphenols at Cerrena unicolor laccase-modified graphite electrode: correlation

between sensitivity and substrate structure, Talanta 66 (2005) 1219–1224, https://doi.org/10.1016/j.talanta.2005.01.026.
[38] R. Fogel, J.L. Limson, Electrochemically predicting phenolic substrates' suitability for detection by amperometric laccase biosensors, Electroanalysis 25 (2013) 1237–1246, https://doi.org/10.1002/elan.201200642.
[39] A. Boujakhrout, S. Jimenez-Falcao, P. Martinez-Ruiz, A. Sanchez, P. Diez, J.M. Pingarron, R. Villalonga, Novel reduced graphene oxide-glycol chitosan nanohybrid for the assembly of an amperometric enzyme biosensor for phenols, Analyst 141 (2016) 4162–4169, https://doi.org/10.1039/C5AN02640G.